





Open Archive Toulouse Archive Ouverte (OATAO)

OATAO is an open access repository that collects the work of Toulouse researchers and makes it freely available over the web where possible

This is an author's version published in: <http://oatao.univ-toulouse.fr/21765>

Official URL: <https://doi.org/10.1149/2.010406eel>

To cite this version:

Patra, Snehangshu and Bruyere, Stéphanie and Taberna, Pierre-Louis  and
Sauvage, Frédéric  *Electrodeposition of TiO₂ Using Ionic Liquids*. (2014) ECS
Electrochemistry Letters, 3 (6). D16-D18. ISSN 2162-8726

Any correspondence concerning this service should be sent
to the repository administrator: tech-oatao@listes-diff.inp-toulouse.fr

Electrodeposition of TiO₂ Using Ionic Liquids

Snehangshu Patra,^{a,b} Stéphanie Bruyère,^a Pierre-Louis Taberna,^{b,c} and Frédéric Sauvage^{a,c,z}

^aLaboratoire de Réactivité et Chimie des Solides, Université de Picardie Jules Verne, CNRS UMR7314, 33 rue Saint-Leu, 80039 Amiens, France

^bRéseau sur le Stockage Electrochimique de l'Energie (RS2E), FR CNRS3459, France

^cUniversité Paul Sabatier, Toulouse III, CIRIMAT CNRS UMR5085, France

We report on the electrodeposition of TiO₂ upon transparent conducting oxide (ITO) by using a milder electrochemical bath based on room-temperature ionic liquids (1-ethyl-3-methyl imidazolium-bis(trifluoromethylsulfonyl)imide) and titanium butoxide as a soluble precursor. By taking advantage of oxygen reduction which proceeds about 500 mV before titanium +IV reduction, well-crystallized thin films of anatase TiO₂ are tailored under potentiostatic control at -1.5 V (vs. AgCl/Ag) / 100°C followed by a rapid post-annealing treatment at 500°C in air.

[DOI: 10.1149/2.010406eel]

The tailoring of nanostructured metal oxide films is at the basis of thorough investigations for both fundamental and applied purposes. The control from the meso- down to the microstructure, the film's texture or the ability to endorse preferentially a given crystal facet; all of these parameters are pooling the challenges to grasp utmost levels of performances. The relationship between the film's characteristics and their functional properties has been scrutinized since a long date in many fields; especially in (photo)-electrochemical devices¹ for (photo)-catalysis² or opto-electronic applications.³ Various methods of fabrication have been considered, from physical high-vacuum deposition to soften low-temperature chemical methodologies. The preference between all these methods is firstly governed by the chemical complexity of the material to grow. Chimie douce methods are often well-adapted to tailor "simpler" binary/ternary oxide systems where the film's nanostructuring impacts the ensuing material properties. The utilization of low temperature processes offers evident advantages to finely control the particles or the film's mesostructure while also being fully compatible with industrial standards for mass production. All these advantages are accessible by the electrodeposition technique with pros and cons. It is a methodology rendering a surface/electrode functional, so far associated with aqueous electrochemical bath. However, the low boiling points of water together with its narrow electrochemical window are two constraints restricting the practical versatility of electrodeposition. Recent researches were prompted toward less conventional media, *eg.* room-temperature ionic liquids (RT-ILs) which hold unprecedented specifications in terms of ionic conductivity, high chemical, electrochemical and thermal stability (>300°C). They were pushed among the most studied media for the last years despite a strong lack of understanding regarding the nature of the chemical/electrochemical active species formed in these liquids. A large branch of materials have been synthesized from noble metals,^{4,5} metals and interrelated alloys⁶⁻⁸ to semi-conductors.⁹⁻¹² The family of imidazolium and pyridinium displays a narrow oxygen, sulfur and iodine solubility paving the way to binary systems.^{8,13-19} Research on the electrodeposition of anatase TiO₂ remains relatively scarce owing to the stability of the Ti³⁺ only maintained to highly acidic aqueous solutions and its high sensitiveness to air.²⁰ In this work, we report for the first time a more adapted and simpler/safer methodology for the electrodeposition of well-crystallized mesoporous films of anatase TiO₂ by using titanium butoxide in conjunction with the 1,3-ethylmethylimidazolium bis(trifluoromethylsulfonyl)imide (EMI.TFSI).

Experimental

Titanium precursors were purchased from Sigma-Aldrich, 99.9% EMI.TFSI from Solvionic and further purified at 75°C in vacuum for 2 days (H₂O content <6 ppm). Prior and during the electrodeposition, the electrochemical bath is saturated with ultra-pure oxygen dehydrated through a P₂O₅ column (Alphagaz).

A three-electrode setup is composed of Asahi ITO glass as working-electrode (WE), Pt gauze as a counter-electrode (CE) and a homemade AgCl/Ag quasi-reference electrode which the potential is -0.09 V vs. Ag⁺/Ag. The electrochemical measurements were carried out using an Autolab PGSTAT30 potentiostat/galvanostat (Eco-Chemie BV). The morphologies were investigated using a scanning electron microscope FEI Quanta200 equipped with EDAX analysis or by transmission electron microscopy using a FEI TECNAI F20S-TWIN 200 kV. A Bruker D8 diffractometer with CuK_α radiation ($\lambda = 1.54056 \text{ \AA}$) was used for film's structural characterization.

Results and Discussion

The first prerequisite to succeed in the electrodeposition of TiO₂ concerns the evaluation of the electrochemical reduction potential of Ti⁴⁺ with respect to O₂²⁻ which can get reduced at once. Indeed, conversely to aqueous chemical bath, in this case the two-electron oxygen reduction will onset the precipitation of the metal oxide at the electrode's surface. It is therefore required to gather two distinct features: (i) a soluble titanium precursor and (ii) the titanium (+IV) reduction should proceed at higher cathodic potentials than solubilized oxygen. Different type of soluble titanium precursors have been investigated (*eg.* chloride, alkoxyde, oxosulfate...). The tetrachloride is the most soluble. The ligand influences drastically the Ti(+IV) reduction as showed the first cycle voltamperogram in EMI.TFSI containing either 0.12M of titanium butoxide (TiOBu) purged or not with oxygen or 0.35M of titanium tetrachloride (concentrations corresponding to the solubility limit) (Fig. 1a). The solubility of oxygen is quantitatively rather comparable to the titanium precursor. Oxygen reduction proceeds according to two steps on ITO, the formation of the stable superoxide anion (O₂⁻) at -1.0 V followed by the less stable peroxide anion (O₂²⁻) at -1.4 V (Figure 1b). Whereas the first electron is reported to be a well-reversible process even though the superoxide anion has about 30 times lower diffusion coefficient than molecular oxygen,²⁰ our results underline the irreversible character of the whole two-electron reduction which accounts for the instable character of the strong nucleophilic peroxide anion electrogenerated. Comparing the reduction wave of oxygen with (Fig. 1a) and without TiOBu (Fig. 1b), the two-step reduction of oxygen is not as well separated in presence of TiOBu. Interestingly, the introduction of TiOBu increases remarkably the oxygen solubility in EMI.TFSI since four times higher current is generated at the electrode ($J_{\text{cath}} = 815 \mu\text{A}/\text{cm}^2$). The integration of this voltamperogram, assuming a strict two-electron process, gives an initial oxygen concentration in the medium of ca. 33 mmol/L (at 100°C) by contrast to the 3.9 mmol/L determined by Buzzeo et al. in pure EMI.TFSI.²¹ Based on our multiple experiences, we argue that TiOBu acts as an oxygen carrier in EMI.TFSI, as similarly to the role played by the artificial perfluorinated compounds developed for abiotic blood substitutes to replace hemoglobin.²²

The second main result concerns the role played by the ligand on the reduction potential of the Ti⁴⁺. In the case of TiCl₄, the reduction

^zE-mail: frederic.sauvage@u-picardie.fr

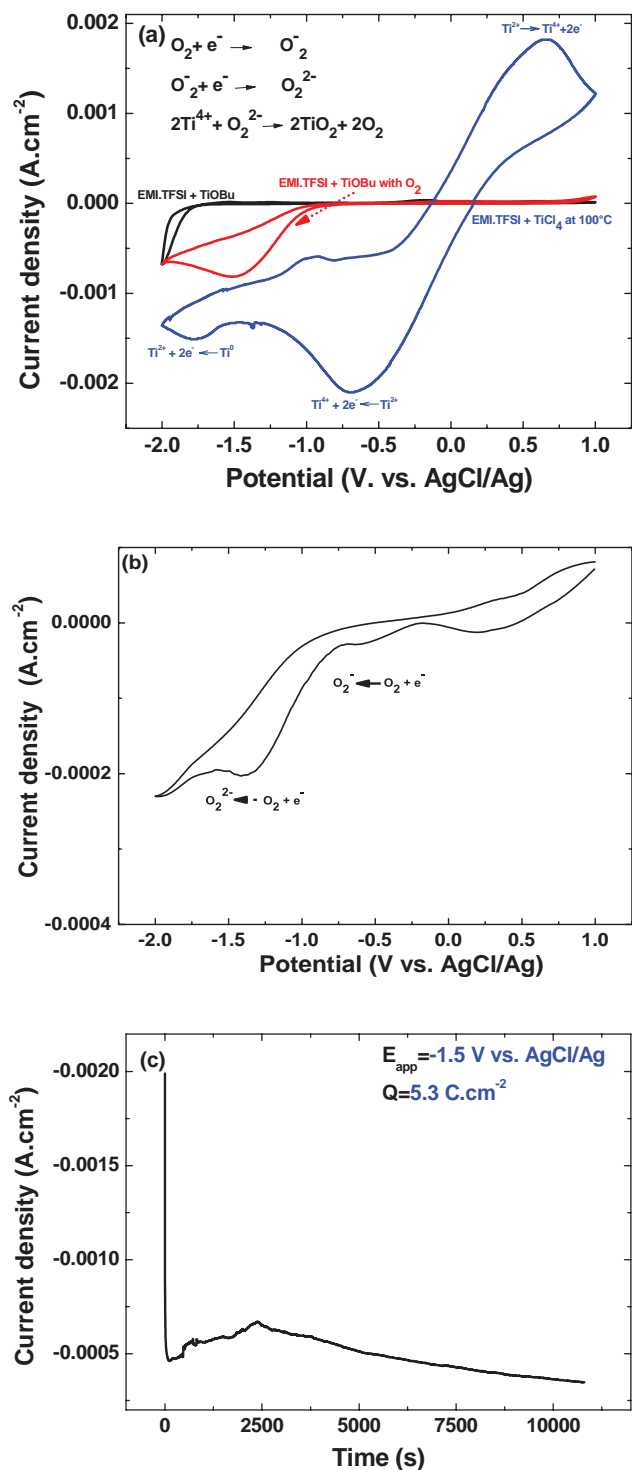


Figure 1. Cyclic voltamperogram recorded at 100°C ($v = 50 \text{ mV.s}^{-1}$) of (a) 0.12M TiOBu in EMI.TFSI (black curve) with electrochemical bath purged of O₂ (red curve) and 0.35M TiCl₄ (blue curve). (b) EMI.TFSI purged with O₂. (c) Typical chronoamperogram recorded at -1.5 V in 0.12M TiOBu in EMI.TFSI at 100°C purged with O₂.

of titanium (+IV) proceeds in two quasi-reversible steps at +0.05 V and -1.65 V, each accounting for two electrons²³ leading to titanium metal.⁹ By contrast, TiOBu reduction gives only one sharp reduction peak at ca. -2.0 V ending up to titanium metal as also suggest the characteristic (J-V) loop corresponding to metal electrodeposition/dissolution. The length of the alkoxyde chain has low effect on the redox potential whereas the greater solubility is obtained with the

longer lipophilic alkyl butoxide chain. The lowest cathodic potential of the alkoxydes suggest that the central titanium cation has a stronger covalent character than for TiCl₄.

The electrodeposition of TiO₂ can thus be achieved using titanium alkoxyde since its reduction proceeds 500 mV below oxygen reduction (Fig. 1a). For the electrodeposition process, we privileged potentiostatic deposition over galvanostatic method to preserve selective reduction of oxygen upon deposition time. The chronoamperogram in Fig. 1c features the typical evolution observed at -1.5 V/100°C for 3 hours. It corresponds to the optimal conditions to reach thin and transparent well-covering film without any trace of IL degradation. Three distinct domains are classically observed: (i) a rapid drop of current, from 2000 to 500 $\mu\text{A.cm}^{-2}$ during the first minute, (ii) followed by a slight current increase to ca. 700 $\mu\text{A.cm}^{-2}$ until ca. 2400s and (iii) a continuous current decrease to ca. 350 $\mu\text{A.cm}^{-2}$. The chronoamperogram integration leads to a charge density of 5.32 C.cm⁻² corresponding to a mass deposited of 2.2 mg.cm⁻² when assuming the peroxide anion to react with Ti⁴⁺ or twice more in case the superoxide anion is involved. Tulodziecki et al. demonstrated that in fact both anions are responsible for ZnO electrodeposition. This would lead to an experimental mass lying between 2.2 and 4.4 mg.cm⁻².¹⁵

The film's morphology is composed of regular spherical particles of 1 μm diameter (Fig. 2a). The topology appears rough including large macropores which can be found along the film depth. EDX analysis confirm the presence of titanium without residues of carbon and fluorine which could have originated from IL degradation or poorly grafted units. Both XRD and TEM analysis reveals that the as-deposited films are amorphous in nature regardless of the applied potential

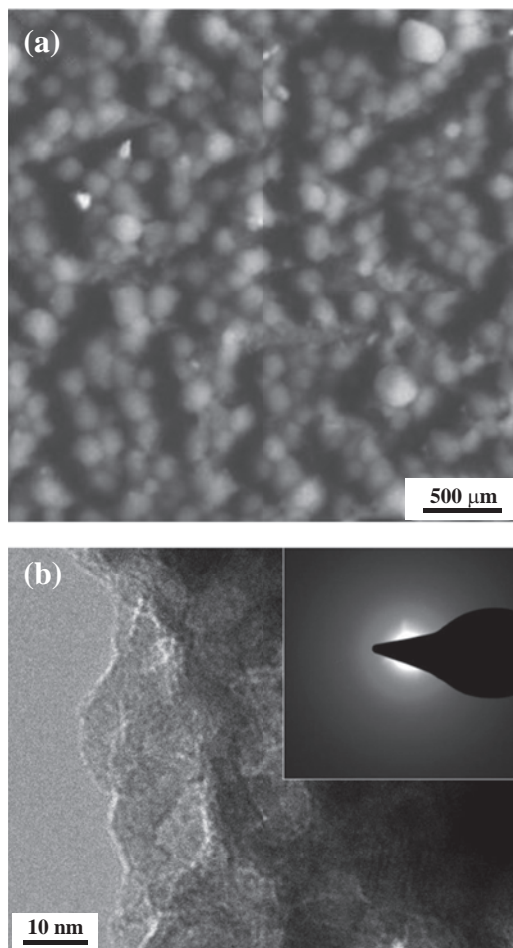


Figure 2. (a) SEM and (b) TEM image of the as-prepared electrodeposited film on ITO obtained by potentiostatic deposition at -1.5 V for 3 hours.

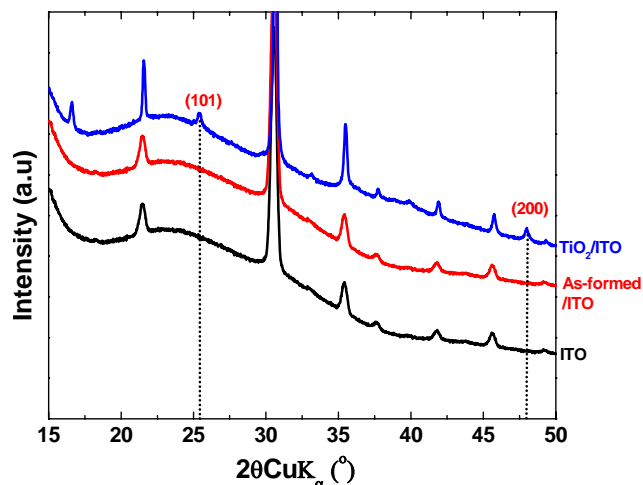


Figure 3. Comparison of the XRD diffractogram before and after air post-annealing at 500°C/5 hours.

($-1.3 \text{ V} < E_{\text{app}} < -1.6 \text{ V}$) and deposition temperature ($< 150^\circ\text{C}$) (Fig. 2b–3). For applied potential equal or below -1.6 V and for temperatures above 120°C , EMI.TFSI degrades yielding on the film's surface globular particles and excessive amount of fluorine and carbon in the film. Since the as-deposited film is X-ray amorphous (Fig. 3), this latter can turn easily crystallized by a rapid post-annealing treatment at 500°C for 5 hours in air. The resulting XRD pattern shows then the growing of two sharp diffraction peaks attributed to the (101) and (200) reflections of the anatase polymorph while exhibiting the characteristic 3.2 eV bandgap energy. The preferential orientation along the [101] direction is not surprising since it corresponds to the low energy facet of the anatase structure.

To conclude, this work reports the first example of anatase TiO_2 electrodeposition using RT-ILs. This was realized throughout a two-step process: potentiostatic electrodeposition at $-1.5 \text{ V}/100^\circ\text{C}$ followed by a rapid post-annealing process entailing the anatase crystallization. This methodology is compatible with a versatile choice of substrates, particularly adequate to non-noble metals and transparent conducting oxide (TCO) glasses as opposed to the aggressive

$\text{TiCl}_3(\text{aq.})$ solution proposed so far. Finally, the results herein presented also highlight one supplementary role of the titanium butoxide which acts as an oxygen carrier, increasing oxygen solubility in the ionic liquid to 33 mmol/L. This preliminary work will pave the way to more in-depth study to control more finely the film morphology, thickness and mesoporosity with the final aim to introduce successfully TiO_2 electrodeposited films for photonic applications.

References

1. F. Sauvage, D. Chen, P. Comte, F. Huang, L.-P. Heiniger, Y.-B. Cheng, R. A. Caruso, and M. Graetzel, *ACS Nano*, **4**, 4420 (2010).
2. Y. Tian, S. R. Bakaul, and T. Wu, *Nanoscale*, **4**, 1529 (2012).
3. A. E. Jimenez and S. G. Santiago, *Semicond. Sci. Technol.*, **22**, 709 (2007).
4. E. Gomez and E. Vallés, *Int. J. Electrochem. Sci.*, **8**, 1443 (2013).
5. B. Dilasari, K. Kwon, C. K. Lee, and H. Kim, *J. Korean Electrochem. Soc.*, **15**(3), 135 (2012).
6. S. Lopez-Leon, R. Ortega-Borges, and G. Brisard, *Int. J. Electrochem. Sci.*, **8**, 1382 (2013).
7. C. Lecoq, J.-M. Tarascon, and C. Guery, *J. Electrochem. Soc.*, **157**(6), A641 (2010).
8. N. Doan, T. Vainikka, E. L. Rautama, K. Kontturi, and C. Johans, *Int. J. Electrochem. Sci.*, **7**, 12034 (2012).
9. C. Fournier and F. Favier, *Electrochem. Commun.*, **13**, 1252 (2011).
10. M. Wu, N. R. Brooks, S. Schaltin, K. Binnemans, and J. Fransaer, *Phys. Chem. Chem. Phys.*, **15**, 4955 (2013).
11. M. Steichen and P. Dale, *Electrochem. Commun.*, **13**, 865 (2011).
12. J. Szymczak, S. Legeai, S. Diliberto, S. Migot, N. Stein, C. Boulanger, G. Chatel, and M. Draye, *Electrochem. Commun.*, **24**, 57 (2012).
13. J. L. Anthony, J. L. Anderson, E. J. Maginn, and J. F. Brennecke, *J. Phys. Chem. B*, **109**, 6366 (2005).
14. E. Azaceta, S. Chavhan, P. Rossi, M. Paderi, S. Fantini, M. Ungureanu, O. Miguel, H. J. Grande, and R. Tena-Zaera, *Electrochim. Acta*, **71**, 39 (2012).
15. M. Tulodziecki, J.-M. Tarascon, P. L. Taberna, and C. Guéry, *J. Electrochem. Soc.*, **159**(12), D691 (2012).
16. C. Arnould, J. Delhalle, and Z. Mekhalif, *J. Electrochem. Soc.*, **156**(11), K186 (2009).
17. Y. Chen, C. Davoisne, J.-M. Tarascon, and C. Guery, *J. Mater. Chem.*, **22**, 5295 (2012).
18. Y. S. Chen, Y. J. Wang, R. Li, J. H. Gu, J. X. Lu, and S. E. Yang, *Chin. Phys. B*, **21**(5), 058801 (2012).
19. H. Y. Huang, D. J. Chien, G. G. Huang, and P. Y. Chen, *Electrochim. Acta*, **65**, 204 (2012).
20. H.-J. An, S.-R. Jang, R. Vittal, J. Lee, and K.-J. Kim, *Electrochim. Acta*, **50**, 2713 (2005).
21. M. C. Buzzo, O. V. Klymenko, J. D. Wadhawan, C. Hardacre, K. R. Seddon, and R. G. Compton, *J. Phys. Chem. A*, **107**, 8872 (2003).
22. K. C. Lowe, *J. Mater. Chem.*, **16**, 4189 (2006).
23. F. Endres, S. Zein El Abedin, A. Y. Saad, E. M. Moustafa, N. Borissenko, W. E. Price, G. G. Wallace, D. R. Macfarlane, P. J. Newman, and A. Bund, *Phys. Chem. Chem. Phys.*, **10**, 2189 (2008).